Biochimica et Biophysica Acta 1851 (2015) 605–619

Contents lists available at ScienceDirect

Biochimica et Biophysica Acta

journal homepage: www.elsevier.com/locate/bbalip

Extra-hepatic metabolism of 7-ketocholesterol occurs by esterification to fatty acids via cPLA2α and SOAT1 followed by selective efflux to HDL

Jung Wha Lee *, Jiahn-Dar Huang, Ignacio R. Rodriguez

Mechanisms of Retinal Diseases Section, Laboratory of Retinal Cell and Molecular Biology, National Eye Institute, National Institutes of Health, Bethesda, MD, USA

ARTICLE INFO

Article history:
Received 25 August 2014
Received in revised form 24 December 2014
Accepted 15 January 2015
Available online 22 January 2015

Keywords:
7-Ketocholesterol
7-Ketocholesterol fatty acid ester
SOAT1
cPLA2α
HDL
Cultured RPE cell

ABSTRACT

Accumulation of 7-ketocholesterol (7KCh) in tissues has been previously associated with various chronic aging diseases. Orally ingested 7KCh is readily metabolized by the liver and does not pose a toxicity threat. However, 7KCh formed in situ, usually associated with lipoprotein deposits, can adversely affect surrounding tissues by causing inflammation and cytotoxicity. In this study we have investigated various mechanisms for extra-hepatic metabolism of 7KCh (e.g. hydroxylation, sulfation) and found only esterification to fatty acids. The esterification of 7KCh to fatty acids involves the combined action of cytosolic phospholipase A2 alpha (cPLA2α) and sterol O-acyltransferase (SOAT1). Inhibition of either one of these enzymes ablates 7KCh-fatty acid ester (7KFAE) formation. The 7KFAEs are not toxic and do not induce inflammatory responses. However, they can be unstable and re-release 7KCh. The higher the degree of unsaturation, the more unstable the 7KFAE (e.g. 18:0 > 18:1 > 18:2 > 18:3 ≫ 20:4). Biochemical inhibition and siRNA knockdown of SOAT1 and cPLA2α ablated the 7KFAE synthesis in cultured ARPE19 cells, but had little effect on the 7KCh-induced inflammatory response. Overexpression of SOAT1 reduced the 7KCh-induced inflammatory response and provided some protection from cell death. This effect is likely due to the increased conversion of 7KCh to 7KFAEs, which reduced the intracellular 7KCh levels. Addition of HDL selectively increased the efflux of 7KFAEs and enhanced the effect of SOAT1 overexpression. Our data suggests an additional function for HDL in aiding extra-hepatic tissues to eliminate 7KCh by returning 7KFAEs to the liver for bile acid formation.

1. Introduction

7-Ketocholesterol (7KCh) is a well-studied oxysterol known for its inflammatory and cytotoxic properties [1]. This oxysterol has been implicated in the pathogenesis of most human age-related chronic diseases [1,2]. It forms by the autooxidation of cholesterol and cholesterol-fatty acid esters (CEs) which are abundantly found in lipoprotein deposits [3]. In the retina, 7KCh has been found associated with lipoprotein deposit in Bruch's membrane and the choriocapillaris [4]. In monkey ocular tissues it was recently reported to accumulate as a process of aging [5]. The levels are particularly pronounced in the retinal pigment epithelium and choriocapillaris (RPE/CH) [5]. In some elderly human RPE/CH tissues and drusen deposits the levels can be comparable to those found in atheromatous plaques [5].

7-KCh is a potent inhibitor of 3-hydroxy-3-methylglutaryl coenzyme A reductase (HMG-CoA reductase), the rate limiting enzyme in cholesterol synthesis, and was briefly investigated as a potential cholesterol lowering drug in rats [6]. This proved short-lived, because the rat liver adapted very quickly and metabolized the orally administered 7KCh into more polar derivatives and bile acids, which were quickly excreted [7]. 7KCh is known to activate hepatic cholesterol 7α-hydroxylase (CYP7A1) [8]. CYP7A1 is the rate-limiting enzyme in bile acid synthesis [9], and its deficiency is known to cause premature atherosclerosis in humans [10]. Other studies by a different group have also demonstrated that dietary 7KCh is very quickly metabolized into bile acids and excreted [8,11]. These investigators concluded that dietary 7KCh is not the source of the 7KCh found in the atherosclerotic plaques [11].

Another enzyme known to metabolize 7KCh is sterol 27-hydroxylase (CYP27A1) [12]. However, *Cyp27A1* −/− null mice had very little difficulty in metabolizing 7KCh into bile acids [13]. Thus, it seems that CYP27A1 is unlikely to be involved in metabolizing dietary 7KCh. Another enzyme that may be involved in the hydroxylation of 7KCh is oxysterol and steroid 7-alpha-hydroxylase (CYP7B1), which is broadly expressed in various tissues [14]. However, disruption of this gene in mice causes no defects in bile acid synthesis [15]. This enzyme seems to be involved in the metabolism of steroids such as androgens and estrogens [16]. This was further confirmed when the CYP7B1 knockout mouse demonstrated sexual development abnormalities [17]. Yet another enzyme reported to be able to metabolize 7KCh is cholesterol sulfotransferase (SULT2B1b) [18]. Another study demonstrated

* Corresponding author at: National Eye Institute, NIH, Mechanisms of Retinal Diseases Section, LRCMB, 6 Center Drive, MSC0608, Bldg. 6 Rm 131, Bethesda, MD 20892, USA. Tel.: +1 301 496 8299; fax: +1 301 402 1883.
E-mail address: leej@nei.nih.gov (J.W. Lee).

http://dx.doi.org/10.1016/j.bbalip.2015.01.007

that by overexpressing SULT2B1b in 293T cells 7KCh-sulfate was formed [19]. However, SULT2B1b is expressed in very low levels in most tissues, and its main function seems to be in regulating adrenal androgens [20]. Thus it seems that the only enzyme that has been clearly demonstrated to metabolize 7KCh is CYP7A1. Unfortunately, this enzyme is only expressed in the liver [21].

In this study we examined the levels of various enzymes that have either been previously reported and/or could potentially metabolize 7KCh in extra-hepatic tissues. We also analyzed by LCMS various metabolites generated from 7KCh in cultured ARPE19 cells as well as tissues with high 7KCh content, such as the retinal pigment epithelium and choriocapillaris [4]. Based on our results we conclude that the main extra-hepatic metabolic pathway for 7KCh is via esterification to 7KCh-fatty acid esters (7KFAEs), by the combined action of cytosolic phospholipase A2 alpha (cPLA2α, to release membrane fatty acids) and sterol O-acyltransferase (SOAT1, esterification to fatty acids). This is followed by efflux to HDL and presumably returning to the liver for bile acid formation and excretion.

2. Materials and methods

2.1. Materials

Cholesterol (Ch) and 7-ketocholesterol (7KCh) were purchased from Steraloids Inc. (Newport, RI). Hydroxypropyl β-cyclodextrin (HPBCD), cholesteryl-fatty acid esters (CEs) and high density lipoprotein (HDL) were purchased from Sigma-Aldrich (St. Louis, MO). Fatty acids, stearic, oleic, linoleic and linolenic were purchased from Thermo Fisher Scientific Inc. (Waltham, MA). Acetonitrile and methanol were purchased from Fisher Scientific (Fair Lawn, NJ). The SOAT1 selective inhibitor (K-604) was a kind gift from Kowa Company Ltd. (Tokyo, Japan). The cPLA2α inhibitor (Cat# 525143) was purchased from EMD Millipore (Billerica, MA). An affinity-purified rabbit anti-SOAT1 polyclonal antibody was purchased from Cayman Chemicals Co. (Ann Arbor, MI) (Cat# 100028). A polyclonal rabbit anti-GAPDH human antibody was purchased from Invitrogen Corp. (Carlsbad, CA). Total RNA from adult human tissues (retina, lung, placenta, brain, liver, kidney, heart, testis, stomach, spleen, small intestines, prostate, and skeletal muscles) was purchased from BD Biosciences (Mountain View, CA). RNA from human skin was purchased from BioChain (Hayward, CA). Total cellular RNA from cultured human RPE cell lines ARPE19 and D407 cells was isolated using TRIzol reagent (Invitrogen Corp., Carlsbad, CA) and purified with RNeasy mini kit (Qiagen, Valencia, CA).

2.2. cDNA synthesis

Concentrations of total RNA were determined by spectrophotometry (Nanodrop ND-100 Spectrophotometer; Biolab, Melbourne, Vic, Australia). Complementary DNA was synthesized from 2 μg of total RNA previously treated with DNase in a 20 μl reaction, using SuperScript III First-strand Synthesis System kit (Invitrogen Corp., Carlsbad, CA). The cDNA from each preparation was diluted 1:5, and 2 μl of each dilution was used for real-time PCR.

2.3. Copy number determination

Expression of mRNAs from CYP7A1, CYP7B1, CYP27A1, CYP46A1, CYP11A1, CH25H and SULT2B1b was quantified by qRT-PCR using SYBR green in an ABI 7500 instrument (Applied Biosystems Inc., Foster City, CA). To measure copy number, plasmid DNA was used to prepare standards. Each gene was amplified from tissue cDNAs with full-length ORF primers and cloned into pcDNA3.1/CT-GFP expression vector. The DNA concentration is measured by A260 and converted to the number of copies using the molecular weight of the DNA. Copy numbers were determined for each test and genes assayed based upon linear regression equations from standard curve assays. Melting curve analysis was performed to confirm production of a single product in each reaction. PCR reactions were performed two independent times in triplicate each time and validated by analysis of template titration and dissociation curves. Table 1 lists the primer pairs for each of the mRNAs quantified in this study. The changes in gene expression were normalized to the 18S ribosomal RNA.

2.4. Relative quantification for qPCR

Quantitative RT-PCR was performed using Taqman ready-to-use primer sets using an AB instrument (ABI 7500; Applied Biosystems, Foster City, CA) according to the manufacturer's specifications. SOAT1 (Hs00162077_m1), SOAT2 (Hs00186048_m1) and cPLA2 (Hs00233352_ml) were measured and normalized to the housekeeping gene GAPD (ABI4352934E). PCR reactions were performed three independent times in triplicate each time.

2.5. Monkey tissue collection

The monkey eyes and tissues were provided by the Pathology Department of the Division of Veterinary Resources after the completion of various NIH-wide protocols. These protocols were unrelated to this study and the tissues were provided as a courtesy to various NIH researchers. Fresh monkey eyes from 6 year old male Rhesus macaques (*Macacca mulatta*) were enucleated within minutes after euthanasia and the eyes were placed on ice.

2.6. Immunoblotting analyses

Monkey tissues and the cultured human RPE-derived cells, ARPE19 and D407, were homogenized in M-PER solution (Pierce, Rockford, IL) containing the Complete® protease inhibitor cocktail (Roche Diagnostics, Mannheim, Germany). Total protein content was determined by the BCA method (Pierce, Rockford, IL). Protein in the cell extract was precipitated using 10% trichloroacetic acid then collected by centrifugation at 15,000 rpm for 20 min at 4 °C. Protein samples (50 μg protein/lane) were separated in 4–12% NuPAGE Novex Bis–Tris Gels running in 1× NuPAGE MOPS SDS Running Buffer at room temperature for 50 min at 200 V (Invitrogen Corp., Carlsbad, CA). The proteins were transferred using Invitrogen iBlot transfer system. Blots were blocked in 1× TBS, pH 7.4, 5% nonfat milk, and 0.05% Tween-20, for 1 h at room temperature and incubated with rabbit anti-SOAT1 human antibody at 1:1000 dilution or rabbit anti-GAPDH human antibody at 1:2000 dilution overnight at 4 °C. The blot was developed using anti-rabbit IgG HRP conjugated secondary antibody at a dilution of 1:20,000 (KPL, Gaithersburg, MD) and imaged on X-ray film using SuperSignal West Pico Chemiluminescent Substrate (Pierce, Rockford, IL).

2.7. Preparation of water soluble 7KCh solution

A 10 mM stock solution was prepared by dissolving the appropriate amount of 7KCh in 1× PBS containing 45% w/v hydroxypropyl-β-cyclodextrin (HPBCD). Briefly, an appropriate amount of 7KCh was dissolved in ethanol and placed in a volumetric flask. The solution of 45% HPBCD is added to 60–70% of the total volume of the flask and sonicated at 45 °C for 1 h. The remainder of the 45% HPBCD is added to the volume of the flask. A 1 mM working solution was prepared by diluting the stock solution ten-fold in 1× PBS.

2.8. Cell culture

ARPE19 cells were obtained from the American Type Culture Collection (Manassas, VA) at passage 22 and grown in DMEM/F12 (1:1, by vol., Mediatech Inc., Herndon, VA) medium containing 10% fetal bovine serum (FBS), 2 mM glutamine, 100 IU/ml penicillin, and 100 μg/ml

Table 1
Primers for qPCR analysis.

Gene name	Forward primer 5′–3′	Reverse primer 5′–3′	Size (bp)	GenBank accession#
CYP7A1	AGAAGGCAAACGGGTGAACC	GGGTCAATGCTTCTGTGCCC	272	NM_000780
CYP7B1	GTGCGTGACGAAATTGACCG	CTCCCTTTCGCACACAGTAGTCC	220	NM_004820
CYP27A1	TCAGCATCTTCTCTGCAGACCGG	TCATTAGCATCCGTGGGAACA	208	NM_005693
CYP46A1	AAGCTGGTGAGCCTGCGC	CGGCAGCTTCTTGTCCTG	88	NM_007121
CYP11A1	CCCTGTTGGATGCAGTGTCT	GACGCTGGTGTGGAACATCT	230	NM_000781
CH25H	TCGACATGATGAACGTCACACTGCT	TAAAGTGAGAGTGATGCAGGTCGTG	186	NM_003956
SULT2B1b	GCTTGTGGGACACCTATGAAG	ATCTCGATCATCCAGGTCGTGC	205	U92315
r18S	ATGCTCTTAGCTGAGTGTCCCG	ATTCCTAGCTGCGGTATCCAGG	101	NR_003286
Beta actin	GATGGTGGGCATGGGTCAGAA	GCTTCTCCTTAATGTCACGCAC	518	NM_001101

streptomycin (all from Invitrogen Corp., Carlsbad, CA). All experiments were done within 10 passages. The D407 (human RPE) cell line was a kind gift from Dr. Richard Hunt (Department of Pathology and Microbiology, University of South Carolina Medical School, Columbia, SC) and were grown in DMEM (Mediatech, Inc, Manassas, VA) supplemented with 4% FBS. All cells were cultured at 37 °C with 5% CO_2.

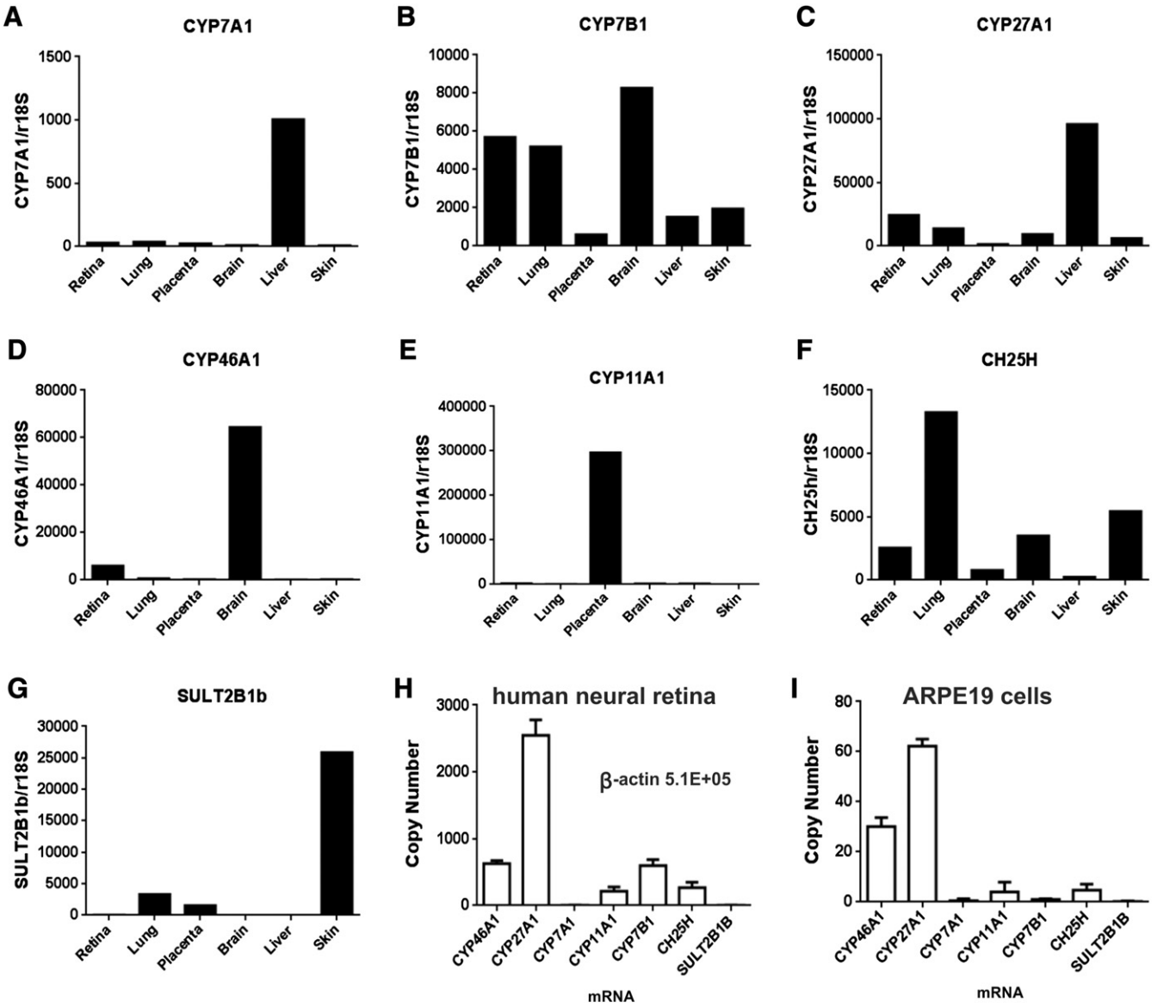

Fig. 1. Measurements of mRNA of several enzymes that could potentially metabolize 7KCh (CYP7A1, CYP7B1, CYP27A1, CYP46A1, CYP11A1, CH25H, SULT2B1b). A–G. mRNA of various enzymes relative to ribosomal 18S in neural retina, lung, placenta, brain, liver and skin. Pooled total RNA prepared from adult human retina (n = 29 & 99), lung (n = 3 & 3), placenta (n = 1 & 1), brain (n = 1 & 1), liver (n = 3 & 3) and skin (n = 1 & 1) was used in this study. PCR reactions were performed two independent times in triplicate each time. H. Copy number of the various enzymes in neural retina. I. Copy number in ARPE19 cells. Data were expressed as means ± SD from three independent experiments. The method used to determine copy number is described in Materials and methods.

2.9. 7KCh treatments

To measure Ch, 7KCh and 7KFAEs inside the cells, ARPE19 cells were seeded in 24-well plates at a density of 150,000 cells per well, in quadruplicate. After reaching 80% confluence, the medium was replaced with fresh serum free medium and 7KCh–HPBCD complex (7K–HPBCD, 0–12 μM) was added directly to the wells containing the cells. This is a critical step. Pre-diluting the 7KCh in the media will significantly reduce the effective dose of 7KCh since it will adhere to the plastic walls of the media container. The cells then were incubated at different time points. At the indicated time, the medium was removed and the cells were washed with PBS three times and Ch, 7KCh and 7KFAEs were extracted using anhydrous ethanol.

2.10. Treatment of SOAT1 inhibitor and cPLA2α inhibitor

ARPE19 cells were pre-incubated with either SOAT1 selective inhibitor (K-604) or Ca^{2+}-dependent-cytosolic phospholipase

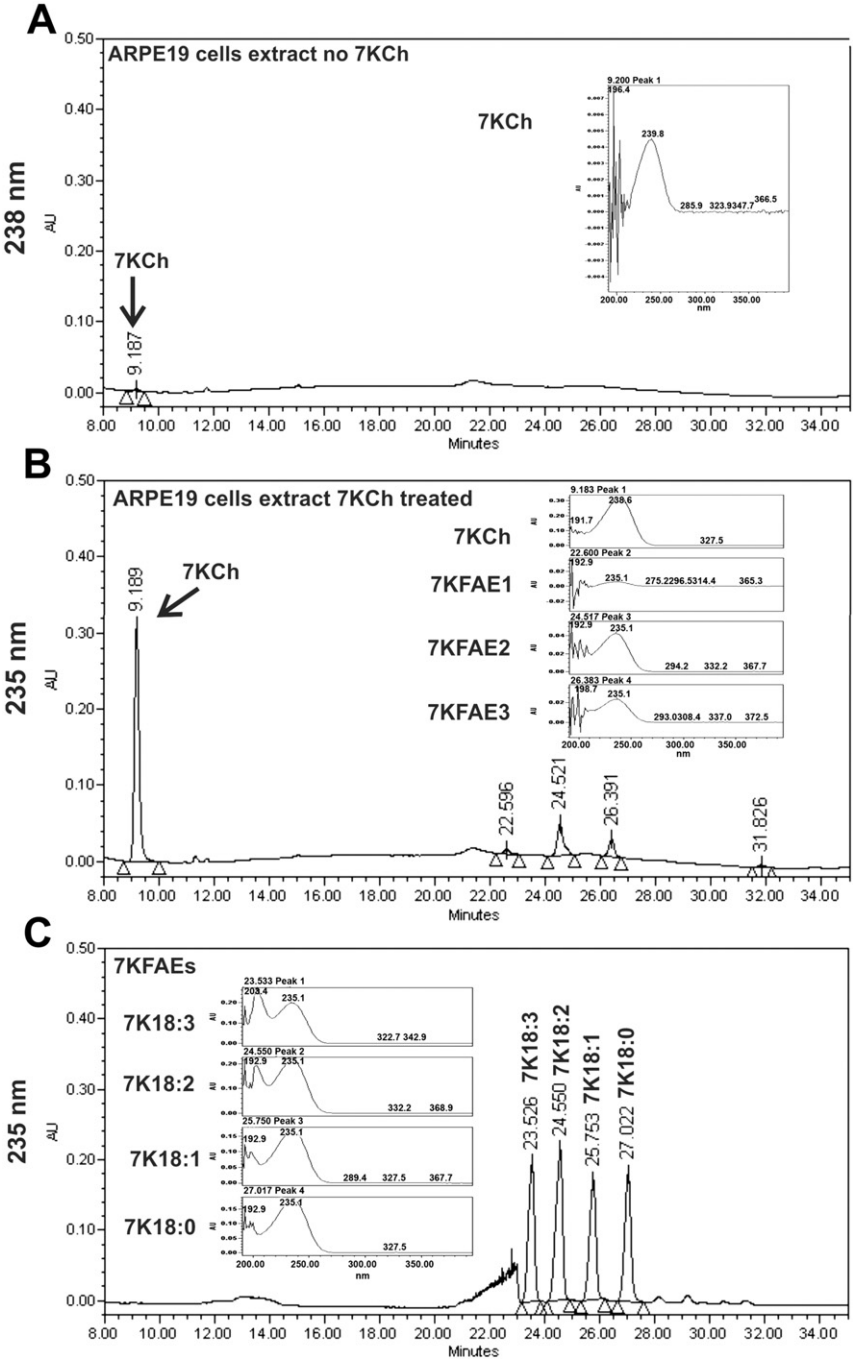

Fig. 2. Measurement of Ch, 7KCh, and 7KFAEs by HPLC with ultraviolet detection (HPLC-UV). Representative chromatographs monitored at 235 nm. A. Extract from untreated ARPE19 cells. B. Extract from ARPE19 cells treated with 8 μM 7KCh for 24 h. C. Chromatograph of four 18 carbon synthetic 7KFAE standards. Insets contain the full spectra of the peaks between 200 and 400 nm.

A2α (cPLA2α) inhibitor (cPLA2α inhibitor) for 1 h prior to 8 μM 7K–HPBCD treatment. After 24 h incubation, the conditioned medium was collected, centrifuged at 1000 rpm for 5 min to remove cell debris, then frozen and stored at −80 °C for the quantification of secreted cytokine levels. Cells were washed three times with PBS and dried at room temperature prior to lipid extraction.

2.11. siRNA knockdown of SOAT1 or cPLA2α

The siRNAs, SOAT1 (SOAT1#6, SI03246803, functionally validated siRNA) and cPLA2α (PLA2GA4#6, SI04140402, Predesigned siRNA) were purchased from Qiagen, Gaithersburg, MD. A nonspecific siRNA (AllStars negative control, catalog number 1027281) was used as a negative control. The efficiency of the silencing was evaluated by qRT-PCR.

To determine whether downregulation of SOAT1 or cPLA2α affected 7KFAE formation and 7KCh-induced inflammation, ARPE19 cells were transfected with siRNA oligos (50 nM) by electroporation using the Nucleofector II instrument (Amaxa Biosystems, Gaithersburg, MD), according to the manufacturer's instructions then allowed to recover for 48 h. After 24 h incubation with 8 μM 7K–HPBCD, the conditioned medium was collected for cytokine assay and cells were collected to measure Ch, 7KCh and 7KFAEs.

2.12. Overexpression of SOAT1

A replication negative adenovirus that induces the overexpression of SOAT1 in transduced cells (AdSOAT1) was purchased from SignaGen Laboratories (Gaithersburg, MD). An adenovirus that expresses enhanced GFP (Vector Biolabs, Philadelphia, PA) was used as a negative

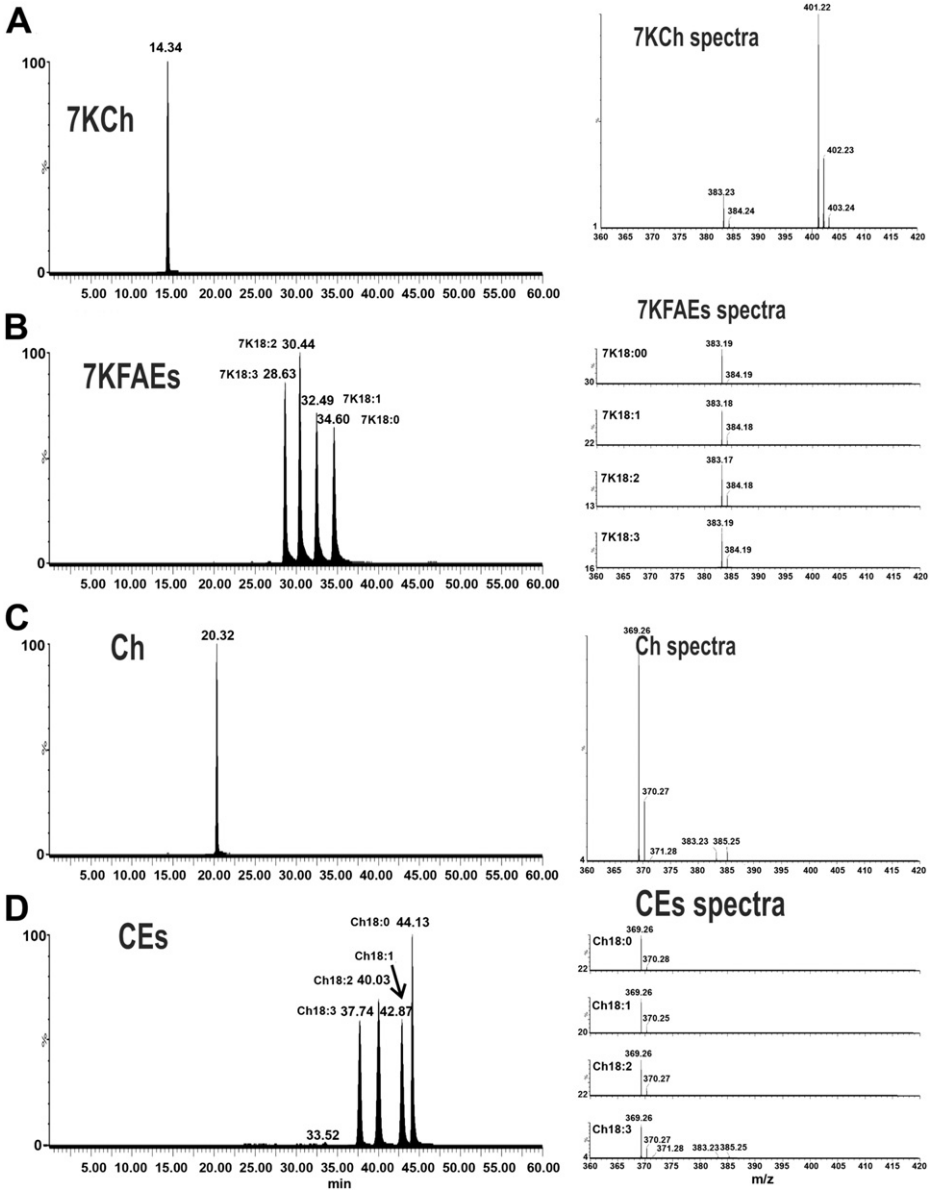

Fig. 3. Measurements of Ch, 7KCh, 7KFAEs and CEs by LCMS. To determine the ions formed and ionization coefficients for the molecules of interest, 500 pmol of each standard was run. A. 7KCh, m/z 401 (M + H, main ion). B. Synthetic 7KFAEs, 7K18:3, 7K18:2, 7K18:1 and 7K18:0. m/z 383 (M-fatty acid, main ion). C. Ch, m/z 369 (M-OH, main ion). D. CEs, Ch18:3, Ch18:2, Ch18:1, and Ch18:0 m/z 369 (M-fatty acid, main ion). The ionization coefficients for the 7KFAEs and the CEs were nearly identical to each other. The average of all four was used to quantify unidentified 7KFAEs and CEs, respectively. Insets show the MS spectra.

control. ARPE19 cells (50,000 cells/well) were seeded onto 24 well plates, grown to 60% confluence, and transduced with AdSOAT1 or AdGFP in serum-free medium (MOI = 20) for 48 h. The efficiency of the overexpression was evaluated by immunoblots. The transfected cells were then treated with 8 μM 7K–HPBCD for 24 h. The conditioned medium was collected to measure cytokine expression levels. Cells were collected for lipid analysis. We did not detect any cell death due to adenovirus transfection at the end of the experiment.

2.13. Cytokine assay in conditioned media

The conditioned media were centrifuged (1000 rpm × 5 min) to remove cell debris and stored at −80 °C until analysis. The levels of IL-1β, IL-6, IL-8 and VEGF protein were measured using the Luminex magnetic bead immunoassay technology following the manufacturer's protocol. Briefly, 25 μl of conditioned medium was added to the pre-wet plate containing 25 μl of assay buffer. To each well, 25 μl of multiple premixed

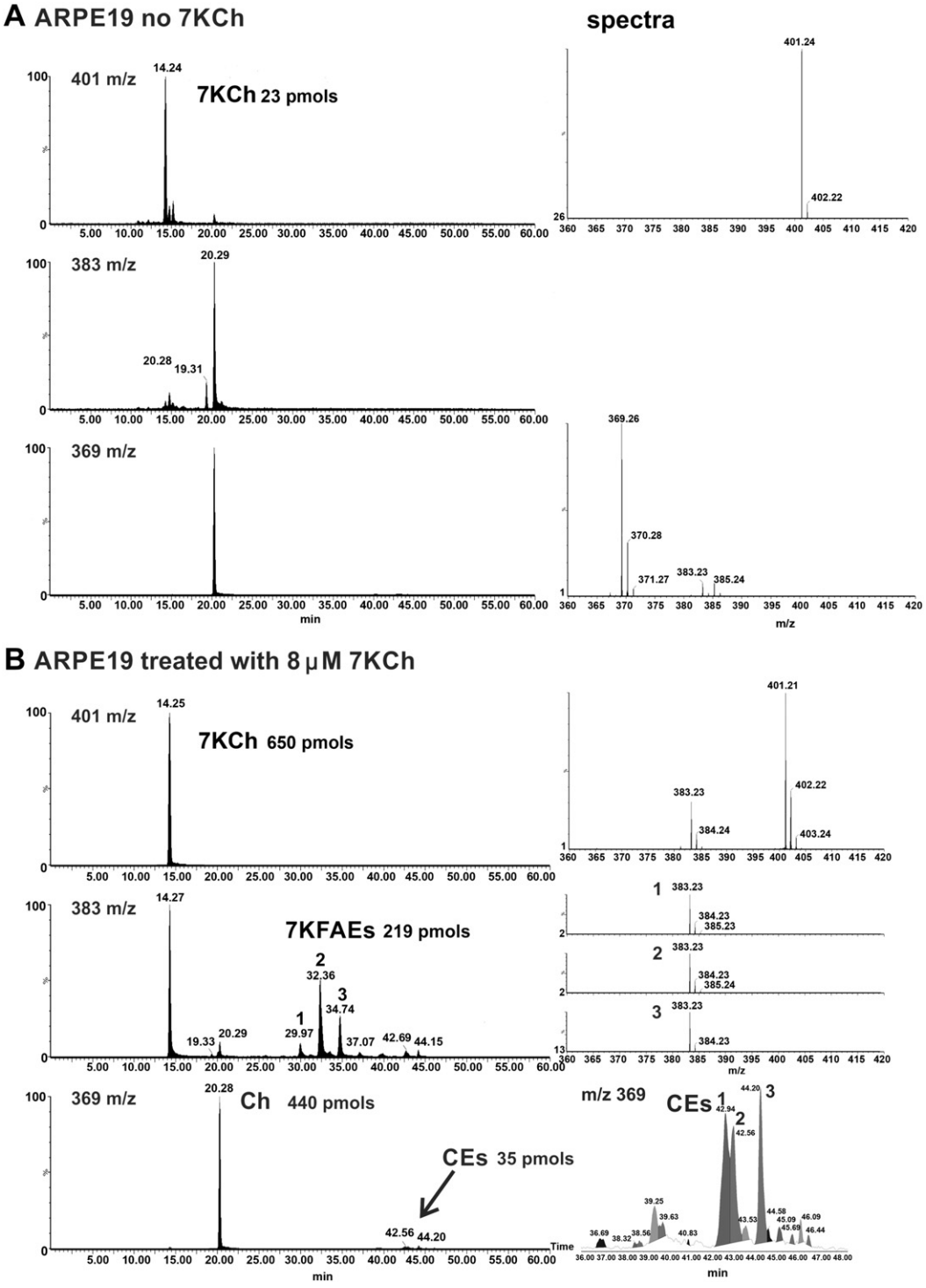

Fig. 4. LCMS analyses of 7KCh treated and untreated ARPE19 cell extracts. The same samples from Fig. 2 were analyzed by LCMS. A. Untreated cells. B. Cells treated with 8 μM 7KCh. Insets demonstrate the MS spectra. Bottom inset demonstrates the m/z 369 ion in the region of CEs. Amounts (pmols) are listed for each component.

microbeads was added, then the plate was sealed with a plate sealer and incubated with agitation on a plate shaker for 18 h at 4 °C. The wells were washed twice with 200 μl Milliplex wash buffer. The beads were shaken with 25 μl of the detection antibody mix for 2 h at room temperature; each antibody is specific to a single cytokine/chemokine. The beads were shaken with 25 μl of the streptavidin–phycoerythrin solution for 30 min at room temperature and washed twice again. The beads were suspended in each well with 150 μl of the Milliplex dry fluid in a shaker for 5 min. The plate was read on MAGPIX Luminex xMAP instrument (Luminex Corp., Austin, TX) and analyzed with Milliplex Analysis software version 3 (EMD Millipore Corporation, Billerica, MA). The concentration of each cytokine was determined using the array reader. A parallel standard curve was constructed for each cytokine. The cytokine levels were normalized to ml of conditioned media volume.

2.14. Cell viability assays

ARPE19 cells were treated with 2–15 μM 7K–HPBCD with or without other compounds for 24 h. Cell viability was measured by cellular dehydrogenase activity using a cell counting kit (Cell Counting Kit-8; Dojindo Molecular Technologies, Gaithersburg, MD). Each measurement was performed in quadruplicate except where noted.

2.15. Synthesis of 7KFAEs

The synthesis of 7KFAEs was reported by Brown et al. [3] and Freeman et al. [22]. However, in this study we synthesized 7KFAEs by the modification of a previous protocol for the synthesis of labeled triglycerides [23]. We have found that this method provides a higher yield and fewer side products. In brief, 0.1 mmol of fatty acid (stearic, 28.4 mg), 0.26 mmol 7KCh (104.1 mg) and 0.12 mmol 4-dimethylaminopyridine (14.6 mg) were weighed. These materials were mixed and dissolved in 0.5 ml of methylene chloride (MeCl) in an ampule. Separately 0.16 mmol N,N-dicyclohexyl carbodiimide (33.0 mg) was weighed and dissolved in 0.5 ml MeCl. Both solutions were mixed in the ampule, flushed with argon gas and then the ampule was sealed. The reaction was allowed to run at room temperature overnight. These proportions were used to synthesize other 7KFAEs. In total four 7KFAEs were synthesized, 7K-18:3 (linolenic), 7K-18:2 (linoleic), 7K18:1 (oleic) and 7K18:0 (stearic). 7KFAEs synthesized from arachidonic (20:4) and decosahexaenoic acids proved to be too unstable in DMSO and ethanol solutions and were not used in this study. The 7KFAEs were purified by preparative HPLC using a tertiary gradient similar to the one used for the analytical quantifications.

2.16. Analyses of Ch, 7KCh, 7KFAEs and CEs

The lipids were extracted by adding 250 μl of dried-ethanol to each well. The ethanol soluble fraction was collected from 4 wells from each sample and evaporated, dissolved in N,N-dimethylformamide (DMF) and injected directly into the LC. Most of the identification and quantification of Ch, 7KCh and 7KFAEs was performed by HPLC-UV. This method is quicker and simpler than by LCMS. In the cases where we also wanted to measure the CE content, LCMS was used since the stronger solvent needed to elute them from the column interfered with their quantification by UV since their UV absorption maxima is around 200 nm.

2.17. HPLC-UV

The HPLC-UV analyses were performed using a Waters 2695 apparatus running Empower 2 software and a 2996 photodiode array detector. The column used was Phenomenex Luna C-8 (3 μm) 2.0 × 250 mm (Torrance, CA) running at 0.25 ml/min. The 7KCh, Ch and 7KFAEs were eluted in a tri-phasic gradient with initial conditions of 25% water and 75% acetonitrile (AcN). The first gradient raised the AcN concentration to 100% in 5 min. This was followed by a second gradient from 100% AcN to 50% AcN, 50% methanol (MeOH) over 15 min. The AcN–MeOH mixture was maintained for another 15 min to elute all of

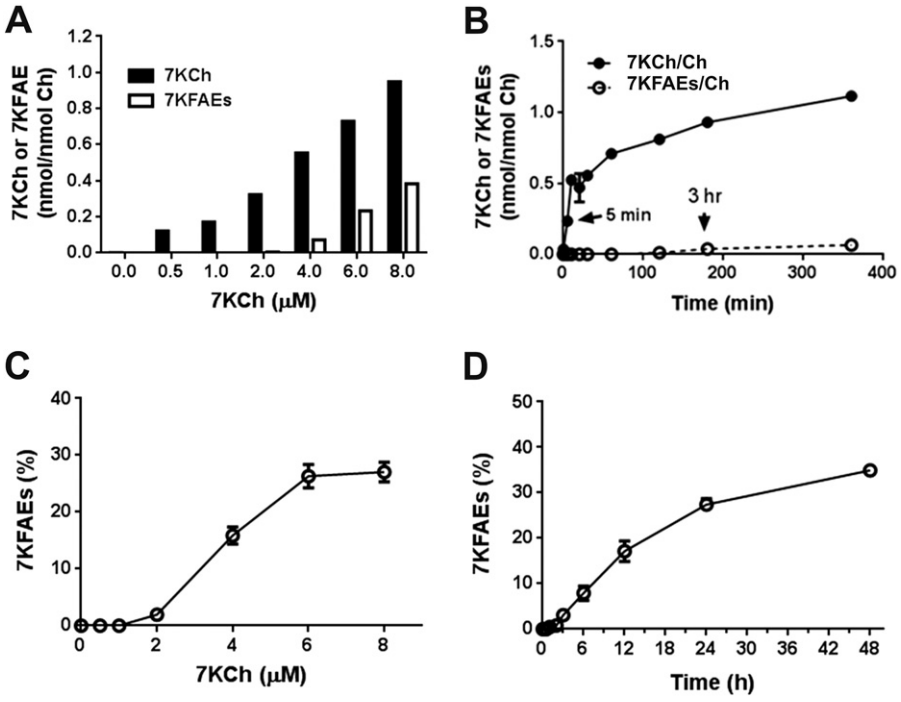

Fig. 5. Kinetics of 7KFAE formation. ARPE19 cells were grown and treated as described above. A. Accumulation of 7KCh and 7KFAEs during 24 h of incubation in various 7KCh concentrations. B. 7KCh accumulation and 7KFAE formation over time (8 μM 7KCh treatment). C. Percentage of 7KCh converted to 7KFAEs in response to increasing 7KCh concentration. D. Percentage of 7KCh converted to 7KFAEs over time (8 μM 7KCh treatment). The 7KFAEs were presented as % of 7KFAEs levels in the cells versus total 7KCh levels (free 7KCh plus 7KFAEs). Data were expressed as means ± SD from three independent experiments.

the 7KFAEs. This was followed by 10 min of re-equilibration to initial conditions for a total of 40 min per run. 7KCh was quantified at 238 nm and Ch at 200 nm using standard curves for each. The 7KFAEs were quantified at 234 nm. The extinction coefficients of the synthetic 7KFAEs were nearly identical, thus the average of the four was used to quantify all 7KFAEs.

2.18. HPLC-mass spectroscopy (LCMS)

Identification and quantification of 7KCh, Ch and the 7KFAEs was also performed by LCMS. The separation was performed using an Agilent 1200 Series HPLC (Santa Clara, CA) equipped with an autosampler and a 1260 Quad pump. The column used was a Varian XRs ultra 2.8 μm, 2 × 100 mm running at 0.15 ml/min. A tri-phasic gradient was used starting with 30% water, 70% AcN to 100% AcN in 15 min. A second gradient was then started from 100% AcN to 100% MeOH to 30 min. A third gradient went from 100% MeOH to 100% MeOH–methylene chloride (50:50 mix) to 40 min. This 3rd gradient is needed to elute the 7KFAEs and the CEs. The re-equilibration takes another 20 min. In the first 5 min the column is flushed with 100% AcN then switched to the starting solvent, 30% water 70% AcN for an additional 15 min. Thus each injection runs for 1 h. The MS used was a Water/Micromass Q-TOF micro using atmospheric pressure ionization in positive mode (APCi+). Masslynx software version 4.1 (Waters, Milford, MA) was used to analyze the data. 7KCh was quantified using the M + H m/z 401 ion and Ch using the M-OH m/z 369 ion as previously described [4]. The 7KFAEs were quantified using the M-fatty acid m/z 383 ion. This is the M-OH 7KCh ion which is also formed in small amounts by 7KCh. The ionization coefficients for the synthetic 7KFAEs were nearly identical. An average of the four was used to quantify all 7KFAEs.

2.19. Statistical analysis

Statistical comparisons between groups were performed using two-tailed Student's *t*-test. We consider the result as significant when $p < 0.05$. Data are shown as means ± SD. All calculations were done using Prism software (GraphPad, San Diego, CA).

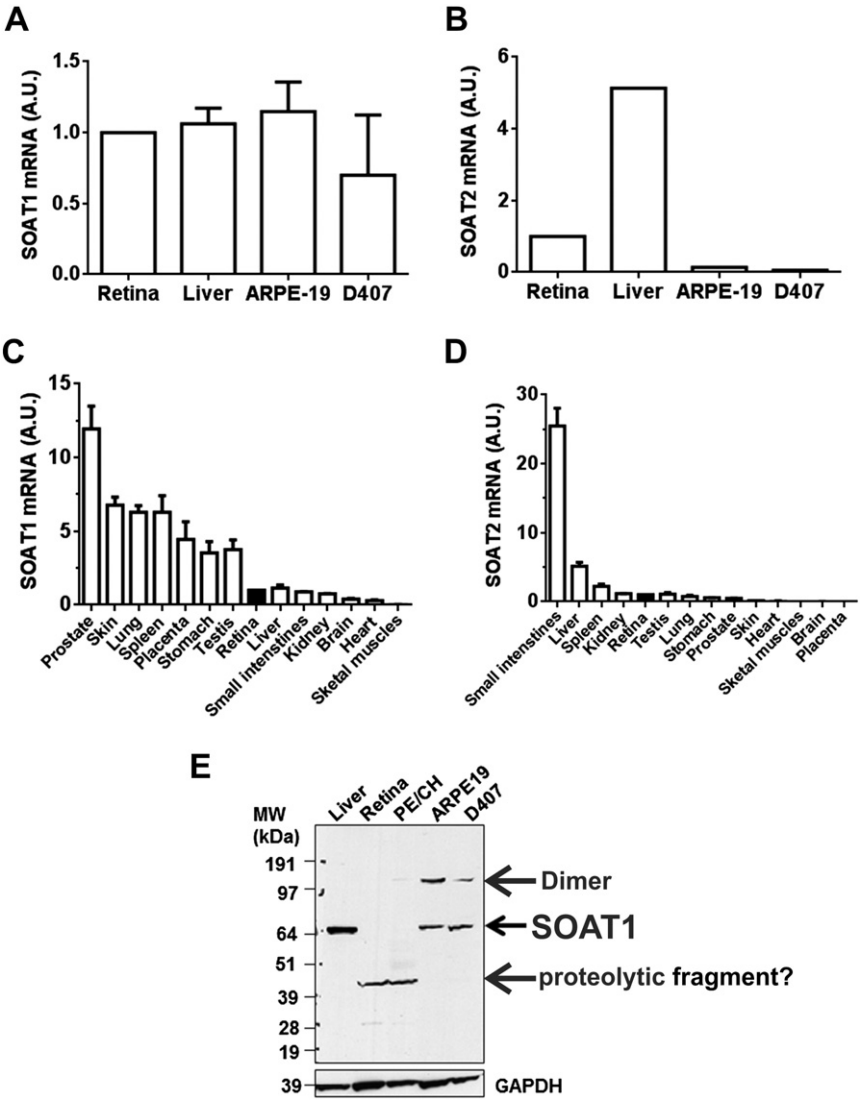

Fig. 6. Expression of SOAT1 and 2 in human tissues. A. Expression of SOAT1 mRNA in human neural retina, liver and the RPE derived cell lines ARPE19 and D407. B. Expression of SOAT2 in the same tissues. C. Expression of SOAT1 mRNA in multiple human tissues. D. Expression of SOAT2 in multiple human tissues. Data were expressed as means ± SD from three independent experiments. E. Immunoblot showing the expression of SOAT1 protein in monkey liver, monkey neural retina, monkey RPE/choroid and the RPE derived cell lines ARPE19 and D407.

3. Results

3.1. Expression levels of various enzymes that could potentially metabolize 7KCh in various human tissues and cultured ARPE19 cells

In order to determine if 7KCh could be metabolized by extra-hepatic tissue we measured the expression (by qRT-PCR) of seven enzymes CYP7A1, CYP7B1, CYP27A1, cholesterol 24-hydroxylase (CYP46A1), cholesterol monooxygenase (side-chain-cleaving) (CYP11A1), 25-cholesterol hydroxylase (CH25H), and SULT2B1b in six human tissues (Fig. 1). As mentioned above, previous studies have shown that CYP7A1 [8,21], CYP27A1 (11), and SULT2B1b [18,19] are capable of metabolizing 7KCh. As previously reported [21] CYP7A1 is liver specific (Fig. 1A). CYP7B1 is broadly expressed [14] but at relatively low levels in all of the tissues tested (Fig. 1B). CYP27A1 is also broadly expressed at low levels with the exception of the liver (Fig. 1C). CYP46A1 is expressed almost exclusively in the brain with about one-tenth (relative to brain) expression in retina (Fig. 1D). CYP11A1 is almost exclusively expressed in placenta (Fig. 1E). CH25H is broadly expressed especially in the lung (Fig. 1F). SULT2B1b is almost exclusively expressed in the skin with much smaller levels in lung and placenta (Fig. 1G) with no detectable expression in the retina. We also measured the mRNA copy number of these enzymes in human neural retina (Fig. 1H) and ARPE19 cells (Fig. 1I). The copy number for all of the enzymes is low as compared to β-actin. CYP27A1 has the highest in both, but SULT2B1b levels are essentially nil.

The low level or complete lack of expression of some of these enzymes (CYP7A1, CYP11A1, and SULT2B1b) suggests that they are unlikely to participate in the metabolism of 7KCh in the retina. However, the moderate level of expression of some of the other enzymes (CYP7B1, CYP27A1, CYP46A1 and CH25H) indicates that they could potentially be involved in the extra-hepatic metabolism of 7KCh in the retina.

3.2. Search for 7KCh metabolites in 7KCh-treated ARPE19 cells

The search for 7KCh metabolites was initially performed by HPLC-UV using lipid extracts from ARPE19 cells that were treated with 7K-Ch. The main differences observed between the untreated (Fig. 2A) and treated cells (Fig. 2B) were the formation of various hydrophobic components with λ_{max} at 235 nm. The identity of these components was immediately known but we suspected, by the significant increase

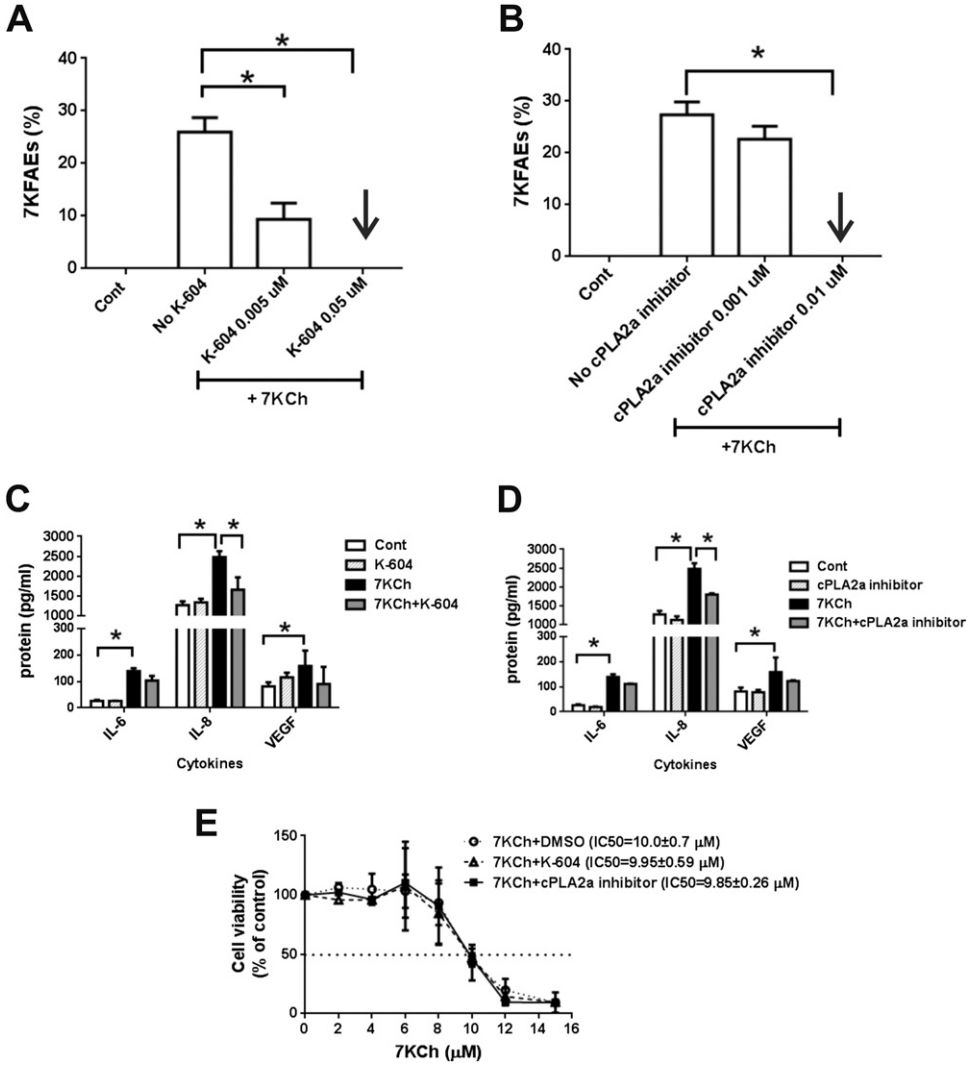

Fig. 7. Effects of SOAT1 and cPLA2α inhibition on 7KCh-induced inflammation and cell death. ARPE19 cells were grown and treated as described above. A. Effect of SOAT1 inhibition with K-604 on 7KFAE formation. B. Effect of cPLA2α inhibition with cPLA2α inhibitor on 7KFAE formation. C. Effect of K-604 treatment on 7KCh-induced cytokine release in conditioned media. IL-6, IL-8 and VEGF were measured as described above. D. Effect of cPLA2α inhibition on 7KCh-induced cytokine release in conditioned media. E. Effect of K-604 or cPLA2α inhibitor on 7KCh-induced cell death. Data were expressed as means ± SD from six independent experiments. *$p < 0.05$ compared to untreated control sample of each group or inhibitor treated group to 7KCh treated of each group.

in retention time, that they were fatty acid esters. These esters are not available commercially, therefore we synthesized four potential esters, 7K18:0 (stearic), 7K18:1 (oleic), 7K18:2 (linoleic) and 7K18:3 (linolenic) as described above. The retention times of the synthetic 7KFAEs were similar to those found in the 7KCh-treated cells and their UV spectra were nearly identical (Fig. 2C).

To further confirm the identity of the 7KFAEs, authentic standards were analyzed by LCMS as described above. 7-KCh generates a main $M + H^+$ ion with m/z of 401. It also forms a minor $M\text{-}OH^+$ ion with an m/z of 383 (Fig. 3A). 7KFAEs also generated an m/z of 383 since the APCi probe fragments the parent molecule and creates an M-fatty acid positive ion (Fig. 3B). Cholesterol (Ch) generates an $M\text{-}OH^+$ ion of m/z 369 (Fig. 3C) with small amounts of $M\text{-}H^+$ (m/z 385). Cholesteryl fatty acid esters (CEs) also generate M-fatty acid ions of m/z 369 (Fig. 3D). The extinction and ionization coefficients of all of the synthesized 7KFAEs and CEs were nearly identical to each other. Hence, we used the average of all four coefficients for quantification of unknown esters.

Analyses of the same samples from Fig. 2 by LCMS revealed similar but more detailed information (Fig. 4). The untreated cell extracts

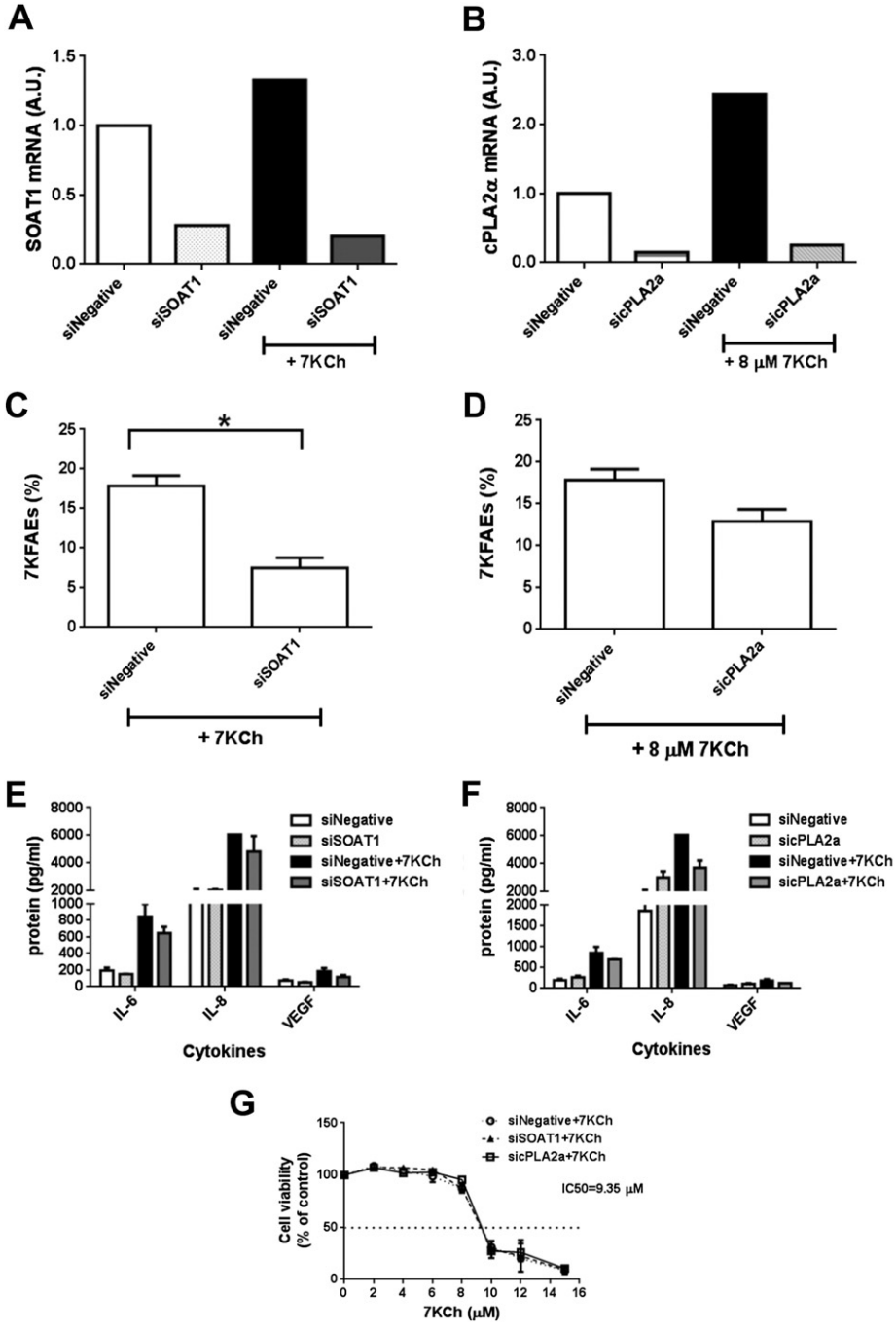

Fig. 8. Effects of siRNA knockdown of SOAT1 or cPLA2α on 7KCh-induced inflammation and cell death. ARPE19 cells were treated with an SOAT1-specific siRNA (siSOAT1) (A, C, E, G) or a cPLA2α-specific siRNA (sicPLA2α) (B, D, F, G) as described above. A. Knockdown of SOAT1 mRNA expression using siSOAT1 versus negative control with and without 7KCh treatment. B. Knockdown of cPLA2α mRNA expression using sicPLA2α versus negative control with and without 7KCh treatment. Data were expressed as mean from two independent experiments in triplicate each time. C. Effect of siSOAT1 on the formation of 7KFAEs. D. Effect of sicPLA2α on the formation of 7KFAEs. E. Effect of siSOAT1 on cytokine levels released into the conditioned media with and without 7KCh treatment. F. Effect of sicPLA2α on cytokine levels released into the conditioned media with and without 7KCh treatment. G. Effect of siSOAT1 and sicPLA2α on 7KCh-induced cell death. Data were expressed as means ± SD from three independent experiments. $^*p < 0.05$ compared to negative siRNA (siNegative) treated group.

contain very small amounts of 7KCh (23 pmol 7KCh/nmol Ch) and no detectable levels of 7KFAEs or CEs (Fig. 4A). The 7KCh-treated sample obviously had a lot more intracellular 7KCh (650 pmol 7KCh/nmol Ch) but also showed m/z 383 peaks consistent with 7KFAEs (Fig. 4B). In addition to the 3 main peaks detected by UV (Fig. 2) the MS detected 4–5 other smaller peaks (Fig. 4B). The combination of the 7KFAEs is approximately 219 pmol (Fig. 4B). More interestingly it also detected a small amount of m/z 369 peaks consistent with CEs. Although these peaks seem insignificant next to Ch (440 pmol), the three main peaks account for 35 pmol (7.4% of total Ch). APCi+ ionization is not ideal for CE detection and the ionization coefficient for CEs is approximately 1/3 that of Ch. However, the CEs are unequivocally detected and not

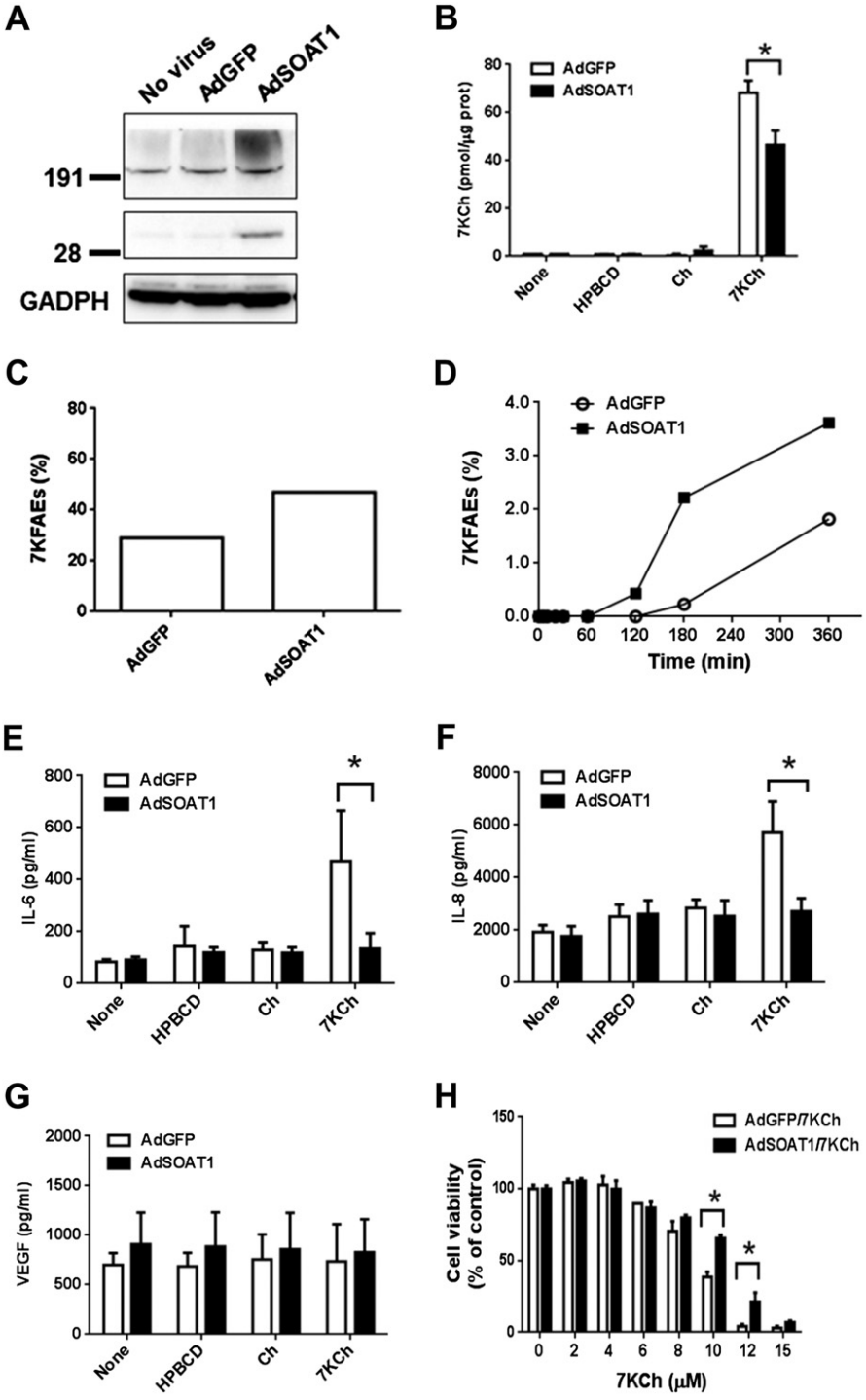

Fig. 9. Effects of SOAT1 overexpression on intracellular 7KCh levels, 7KFAEs synthesis, 7KCh-induced cytokine release and cell death. ARPE19 cells were transduced with a replication negative adenovirus containing SOAT1 (AdSOAT1) as described above. A. Immunoblot developed with anti-SOAT1 antibodies demonstrating SOAT1 overexpression in ARPE19 cell protein extracts. B. Effect of AdSOAT1 transduction on intracellular 7KCh levels (mean ± S.D., $n = 4$). The levels were normalized to proteins. $^{*}p < 0.05$ compared to AdGFP transduced group. C. Effect of AdSOAT1 transduction on 7KFAE synthesis. D. Effect of AdSOAT1 transduction on the rate of 7KFAEs synthesis. Data were expressed as means ± SD from three independent experiments. The levels of IL-6, IL-8 and VEGF were measured in the conditioned media from ARPE19 cells treated with HPBCD (carrier), Ch and 7KCh with and without AdSOAT1 transduction. Experimental details are described above. E. Effect of AdSOAT1 on IL-6. F. Effects of AdSOAT1 on IL-8. G. Effect of AdSOAT1 on VEGF. H. Effect of AdSOAT1 on 7KCh-induced cell death. Data were expressed as means ± SD from three independent experiments. Each measurement was performed in duplicate.

present in untreated cells. This suggests that 7KCh may be stimulating an enzyme that also generates CEs. This may also be the reason Ch levels drop in response to 7KCh treatment.

We have also searched for hydroxylated and sulfated forms of 7KCh in 7KCh-treated ARPE19 cells as well as in monkey and human RPE/choroid tissue which have significant levels of 7KCh [4,5]. We have not found any detectable levels of hydroxylated or sulfated forms of 7KCh (data not shown). There were detectable levels of 7-hydroxycholesterol (7HCh). This oxysterol is formed by the same mechanism as 7KCh and will further oxidize to 7KCh. In the human and monkey RPE/choroid tissue, aside from significant amounts of 7KCh, 7HCh and CEs, we also detected very small amounts of 24- and 27-hydroxycholesterol (data not shown). However, these two oxysterols are present in blood and may be the reason they were found in the RPE/choroid tissue. The choriocapillaris is impossible to dissect free of blood without perfusion prior to euthanasia and dissection.

The formation of 7KFAEs and the small but detectable increase in CEs led us to suspect the involvement of SOATs since these enzymes are known to synthesize CEs [24].

3.3. Kinetics of 7KFAE formation

In order to better understand how 7KCh interacted with the ARPE19 cells and the process of 7KFAE formation, several experiments were performed to determine the concentration range and time needed for synthesis.

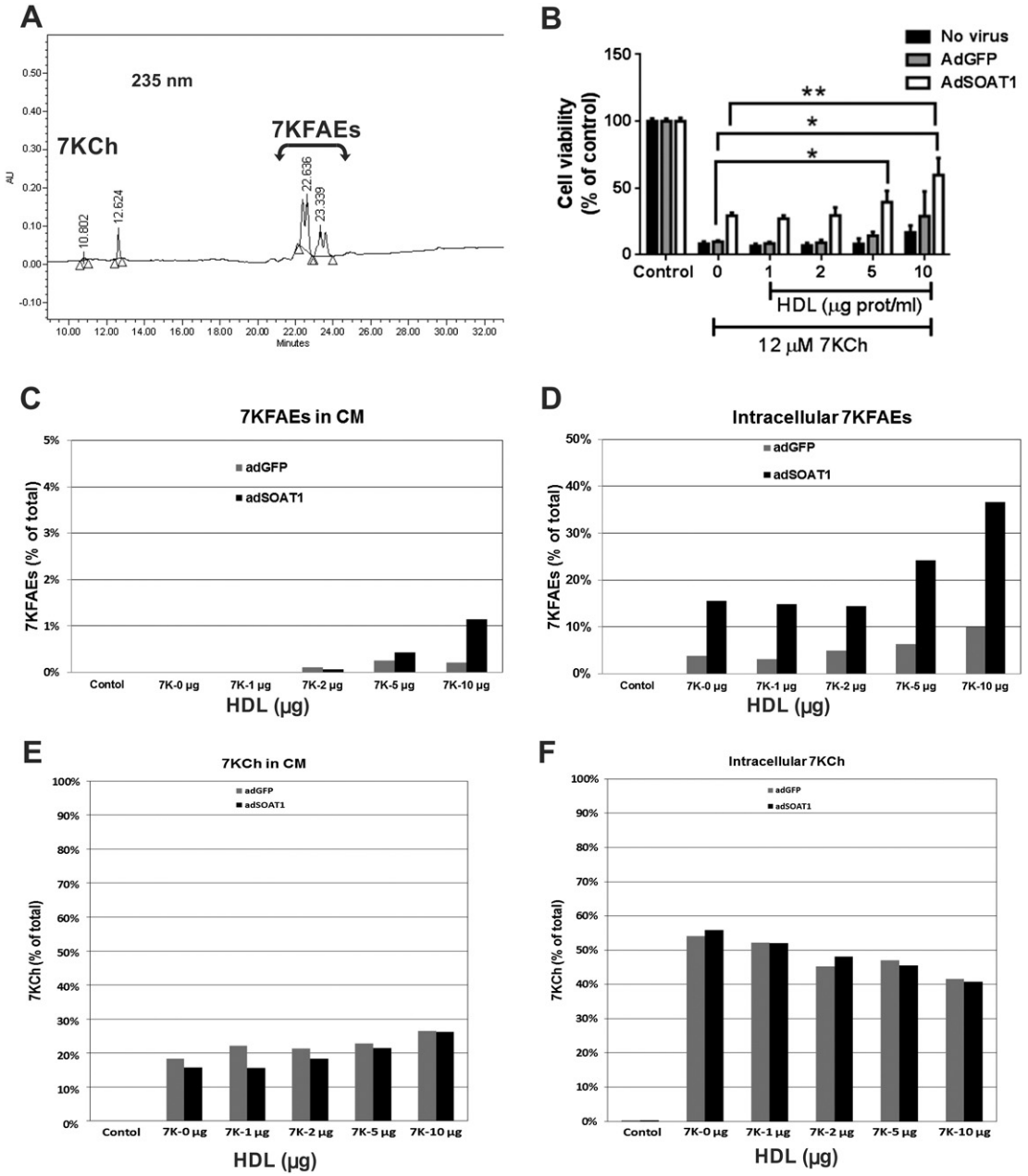

Fig. 10. Effect of HDL on 7KFAE efflux. ARPE19 cells were treated with the increasing amounts of HDL (1–10 μg) in the presence of 7KCh (12 μM) as described above. A. HPLC-UV analysis of commercially available HDL. B. Effect of increasing amounts of HDL on 7KCh-induced cell death with and without AdSOAT1 transduction. Data were expressed as means ± SD from three independent experiments. Each measurement was performed in duplicate. *$p < 0.05$ compared to AdGFP transduced group. **$p < 0.05$ compared to AdSOAT1 transduced group without HDL treatment. C. Effect of HDL on the efflux of 7KFAEs into the conditioned media with and without AdSOAT1 transduction. D. Effect of HDL on intracellular levels of 7KFAEs with and without AdSOAT1 transduction. E. Effect of HDL on the efflux of 7KCh into the conditioned media with and without AdSOAT1 transduction. F. Effect of HDL on intracellular levels of 7KCh with and without AdSOAT1 transduction.

ARPE19 cells were treated with 7KCh in concentrations ranging from 0–8 μM. Doses above 8 μM are lethal within 24 h and 4 μM is needed to initiate an inflammatory response [25]. The 7KFAEs were quantified by LC-UV as described above. Values are normalized to cholesterol (Ch). The results indicate that 7KFAEs are not synthesized until 7KCh levels are at 2 μM or above (Fig. 5A). At 8 μM 7KCh reaches a 1:1 ratio with cholesterol (Fig. 5A) and this takes approximately 3 h (Fig. 5B). Approximately 25–30% of the internalized 7KCh is converted to ester if 7KCh is given in doses above 6 μM (Fig. 5C). The 7KFAE synthesis continues steadily for 24 h but changes little between 24 and 48 h (Fig. 5D).

Thus, to reach the maximum level of 7KFAE formation it requires 6–8 μM 7KCh and about 24 h. The capacity to store the 7KFAEs seems to saturate after 24 h of 7KCh exposure.

3.4. Expression of SOAT1 and 2 in cultured cells and human tissues

As mentioned above, the enzymes most likely to be involved in the synthesis of 7KFAEs would be the SOATs [26]. SOATs are known to synthesize cholesterol fatty acid esters using fatty acids released from membrane phospholipids [24]. There are two known SOATs, SOAT1 and SOAT2. To determine the involvement of the SOATs in the synthesis of 7KFAEs, their mRNA expression was measured (by qRT-PCR) in human retina, liver and in two RPE-derived cultured cells, ARPE19 and D407 (Fig. 6A, B). SOAT1 was expressed in roughly equal levels in the four tissues tested (Fig. 6A). SOAT2 was highly expressed in human liver, but there was little expression in human retina and it was barely detectable in the cultured cells (Fig. 6B). We then examined their expression in a variety of human tissues (Fig. 6C, D). SOAT1 is expressed in most tissues (Fig. 6C), while SOAT2 seems to be more selective (Fig. 6D) as previously reported [27]. SOAT2 is almost exclusively expressed in the small intestines and liver. Since there is little expression of SOAT2 in retina and in the RPE-derived cell lines, all of the subsequent work was focused on SOAT1.

At the protein level immunoblots show that SOAT1 is expressed in monkey liver. The two RPE-derived cell lines express the full size protein (MW: 65 kDa) and possibly a dimer (Fig. 6E) [28]. Human retinal tissue is difficult to obtain without considerable postmortem time, therefore monkey retina was used. The monkey retina and RPE/choroid tissues express a smaller fragment which may be due to proteolysis in the sample (Fig. 6E).

3.5. Inhibition of SOAT1 and its partner cytosolic phospholipase 2A (cPLA2α)

Initially we investigated cPLA2α because of its connection to inflammation. This enzyme is known to release arachidonic acid, which is the precursor for prostaglandins and leukotrienes [29]. However, it soon became evident that cPLA2α was working with SOAT1 to form the 7KFAEs [22].

To determine if these two enzymes were indeed responsible for the formation of the 7KFAEs and potentially mediate the 7KCh-induced inflammation, we inhibited their function using K-604 (SOAT1) and cPLA2α inhibitor (cPLA2α) in 7KCh treated ARPE19 cells (Fig. 7). Inhibition of SOAT1 (Fig. 7A) and cPLA2α (Fig. 7B) ablated the 7KFAE formation. This inhibition had no significant effect on the 7KCh-induced cytokine release (Fig. 7C, D) or on protecting the cells from 7KCh-induced cell death (Fig. 7E). Both inhibitors demonstrated a statistically significant drop in IL-8. However, we have no other evidence to suggest that the cPLA2α and SOAT1 are involved in mediating any of the 7KCh-induced inflammatory responses. Other work from our group has shown that most of the 7KCh-induced inflammatory and cell death responses are mediated by the activation of the Toll-like receptor 4 (TLR4) [30].

3.6. Knockdown of SOAT1 and cPLA2α using siRNAs

Since inhibitors may at times have other non-specific properties, we wanted to further demonstrate the involvement of SOAT1 and cPLA2α on the synthesis of 7KFAEs by a different method. We used siRNAs to knock down the mRNA expression of SOAT1 and cPLA2α and measured the effect on the 7KFAE synthesis, cytokine production and cell viability (Fig. 8).

ARPE19 cells were transfected with an SOAT1 and a negative control siRNA as described above. The siRNA knockdown of SOAT1 was very effective and was not affected by 7KCh treatment which causes a slight induction of SOAT1 mRNA (Fig. 8A). The knockdown of SOAT1 did have a significant effect on the reduction of 7KFAE synthesis (Fig. 8C). However, as with the inhibitors it had little effect on the cytokine inductions (Fig. 8E). The SOAT1 knockdown also failed to protect the cells from 7KCh-induced cell death (Fig. 8G).

An identical series of experiments using a cPLA2α siRNA yielded very similar results (Fig. 8B, D, F, G). The siRNA was very effective at reducing the cPLA2α mRNA levels even though 7KCh does cause a significant induction (Fig. 8B). The cPLA2α siRNA caused only a moderate reduction in 7KFAE synthesis (Fig. 8D). It had little or no effect on the 7KCh-induced cytokine production (Fig. 8F) and also failed to protect cells from 7KCh-induced cell death (Fig. 8G).

The siRNAs were not as effective as the inhibitors at reducing SOAT1 and cPLA2α activities (Fig. 7). This is likely due to the existing levels of these enzymes present in the cells and their relatively slow turnover. However, the effects were consistent with those caused by the inhibitors (Fig. 7).

3.7. Overexpression of SOAT1

The inhibition or knockdown of SOAT1/cPLA2α had no significant biological effect on 7KCh-induced inflammation and cell death. To further investigate this effect overexpression of SOAT1 was performed by transducing ARPE19 cells with a commercially available replication negative adenovirus (AdSOAT1) as described above. A similar adenovirus overexpressing GFP was used as a negative control (AdGFP). The immunoblot indicates that there is a significant level of overexpression in the AdSOAT1 transduced cells but most of the immunoreactive protein is an amorphous aggregate of various molecular weights (Fig. 9A) as previously reported [31]. After transduction the cells were treated with 8 μM 7KCh and the levels of 7KCh, Ch and 7KFAEs were quantified by LCMS. The overexpression caused a significant drop in intracellular 7KCh (Fig. 9B) and a significant increase in intracellular 7KFAEs (Fig. 9C). It also altered the kinetics of 7KFAE formation by significantly increasing the rate of synthesis (Fig. 9D). More importantly, SOAT1 overexpression significantly reduced the 7KCh-induced expression of IL-6 (Fig. 9E) and IL-8 (Fig. 9F) but had no effect on VEGF (Fig. 9G). Interestingly, it provided a moderate but statistically significant level of protection from 7KCh-induced cell death (Fig. 9H).

This positive effect caused by the SOAT1 overexpression is likely due to the significant reduction of intracellular 7KCh levels below the threshold that induces inflammation and cytotoxicity.

3.8. HDL increases 7KFAE efflux and protects cells from 7KCh-induced cell death

While performing HPLC analyses on commercially purchased HDL and LDL samples, we observed that HDL contained (aside from Ch and CEs) a small amount of 7KCh and other components that we recognized as 7KFAEs (Fig. 10A). LDL by contrast contains much higher levels of CEs (approximately 60% of total Ch) but no 7KFAEs (data not shown). This suggested that the missing element in the extra-hepatic 7KCh metabolism may be HDL.

The ARPE19 cells were treated with a lethal dose of 7KCh (12 μM) in combination with different amounts of HDL in the media with and

without SOAT1 overexpression (Fig. 10B). The results indicate that SOAT1 overexpression protects the cells but this protection is enhanced by the presence of HDL at 5 μg/ml and higher (Fig. 10B).

To determine if this protection is occurring due to 7KCh and 7KFAE efflux to HDL, lipid extracts from the samples in Fig. 10A were analyzed by LCMS. The presence of HDL in the conditioned media (CM) significantly increased the levels of 7KFAEs in the CM (Fig. 10C) but no significant change in 7KCh levels was observed (Fig. 10D, E).

Interestingly, the intracellular levels of 7KFAEs also increased in the presence of HDL (Fig. 10D) suggesting HDL may be further stimulating their synthesis. This suggests that HDL preferentially effluxes 7KFAEs. The intracellular levels of 7KCh were decreased in a dose-dependent manner in both cells with and without SOAT1 overexpression (Fig. 10F).

This data suggests that HDL can function not only in returning excess CEs to the liver but it can also aid in removing 7KCh in the form of 7KFAEs from extra-hepatic tissues.

4. Discussion

7-KCh accumulates in significant levels in the back of the retina [4,5]. It is associated with lipoprotein deposits and other lipid debris that accumulates in Bruch's membrane and the choriocapillaris as a consequence of aging [4,5,32]. This 7KCh accumulation is suspected of causing a chronic inflammatory response that in some individuals could initiate the pathogenesis of age-related macular degeneration [1]. In human and drusen samples from elderly donors the accumulation can reach mM levels [5], which leads us to suspect that most of the 7KCh is sequestered in lipoprotein deposits and not readily available to the surrounding tissues. However, it is likely that any tissue in the vicinity of those 7KCh-laden deposits will likely be in a chronic stage of inflammation and at risk of receiving a lethal dose.

In this study we investigated various potential pathways for extra-hepatic 7KCh metabolism. Our data suggests that hydroxylation and/or sulfation are not likely to be involved in any significant way (Figs. 1–4). The rationale for this is two-fold; 1) we cannot find any of the hydroxylated or sulfated metabolites, 2) the enzymes that could potentially perform these reactions are either completely absent (CYP7A1, CYP11A1, SULT2B1b) or expressed at relatively low levels (CYP7B1, 27A1, 46A1) in the retina and/or in most extra-hepatic tissues. The two best candidates CYP27A1 and CYP46A1 could form 27-hydroxy-7KCh and 24-hydroxy-7KCh. However, we failed to detect these two compounds in cultured cells treated with 7KCh as well as in monkey and human samples of RPE/choroid tissues which contained very high levels of 7KCh [4,5]. The only 7KCh derivatives that we have detected are the 7KFAEs (Figs. 2–4). These are readily detected in lipid extract from 7KCh treated cells and commercially available HDL. In the RPE/choroid of monkey and human samples we readily detect 7KCh, 7HCh (which is epimeric), Ch and CEs but generally no 7KFAEs [4,5].

We hypothesize that there are two main reasons that explain the lack of 7KFAEs in biological samples (except HDL). First, the 7KFAEs cannot form from CE-rich deposits. Most CEs in lipoprotein deposits contain polyunsaturated fatty acids which will oxidize simultaneously with Ch during autooxidation (Fenton reaction). This will generate a complex mixture of molecules that will break apart the ester bond leaving the oxidized cholesteryl moiety further oxidizing mostly to 7KCh and the oxidized fatty acids. The second reason, as we have observed during the synthesis and manipulation of 7KFAEs, is that they are unstable. The higher the degree of unsaturation, the more unstable the 7KFAE. Therefore, the fate of the oxidized CEs in lipoprotein deposits is the formation of mostly 7KCh (from the cholesteryl moiety) and oxidized fatty acids. The oxidized fatty acids are significantly more soluble than 7KCh and will likely leech out into circulation over time and be cleared by the kidneys. In monkeys and especially humans this is a process that can take many decades and is unique (in terms of time and degree of oxidation) to each individual. Therefore, the 7KFAEs observed in HDL with unoxidized fatty acids moieties are likely those synthesized by the cPLA2α/SOAT1 using unoxidized membrane fatty acids.

Our data suggests that HDL can selectively remove 7KFAEs from cells. Low doses of HDL (5–10 μg/ml) can significantly protect cells from 7KCh-induced cell death, especially when 7KFAE formation is enhanced by the overexpression of SOAT1 (Fig. 10). The presence of significant levels of 7KFAEs in commercially available HDL suggests that this may be the pathway for returning 7KCh to the liver, which seems to be the only tissue that can properly detoxify 7KCh. To our knowledge this is a novel function for HDL.

The benefits of high HDL levels and its role in the "reverse cholesterol" pathways have been well documented [33]. HDL is known as the "good" cholesterol while LDL, which is a much larger particle highly enriched in CEs, is considered the "bad" cholesterol [33]. HDL in combination with the cholesterol ester transfer protein (CETP) moves CEs to and from LDL. The HDL containing CEs returns to the liver where Ch is converted into bile acids and excreted. Our data suggests that HDL may also help cells that are in contact with oxidized LDL deposits with high levels of 7KCh, to efflux the 7KFAEs synthesized via the cPLA2α/SOAT1 (Fig. 10). As we have shown in our in vitro model, this reduces the inflammatory response, and helps preserve cellular function and viability.

In summary, there is no "real" extra-hepatic metabolism of 7KCh. The formation of 7KFAEs is not the main function of cPLA2, SOAT1 and HDL. Accumulation of lipoprotein deposits and subsequent oxidation occurs late in life and this pathway has not benefited from natural selection. Thus, in its present form this is an inefficient and insufficient pathway to clear 7KCh from lipoprotein deposits. This is an example of cells using available resources to deal with a problem (7KCh accumulation) they are not evolutionarily equipped to handle. However, this study does provide additional insight into how extra-hepatic tissues are handling 7KCh accumulation and how HDL may be aiding in 7KCh elimination.

Transparency document

The Transparency document associated with this article can be found, in the version.

Acknowledgements

This work was supported by the National Eye Institute Intramural Research Program.

References

[1] I.R. Rodriguez, I.M. Larrayoz, Cholesterol oxidation in the retina: implications of 7-ketocholesterol formation in chronic inflammation and age-related macular degeneration, J. Lipid Res. 51 (2010) 2847–2862.
[2] G. Poli, F. Biasi, G. Leonarduzzi, Oxysterols in the pathogenesis of major chronic diseases, Redox Biol. 1 (2013) 125–130 (Review).
[3] A.J. Brown, R.T. Dean, W. Jessup, Free and esterified oxysterol: formation during copper-oxidation of low density lipoprotein and uptake by macrophages, J. Lipid Res. 37 (1996) 320–335.
[4] E.F. Moreira, I.M. Larrayoz, J.W. Lee, I.R. Rodriguez, 7-Ketocholesterol is present in lipid deposits in the primate retina: potential implication in the induction of VEGF and CNV formation, Invest. Ophthalmol. Vis. Sci. 50 (2009) 523–532.
[5] I.R. Rodriguez, M.E. Clark, J.W. Lee, C.A. Curcio, 7-Ketocholesterol accumulates in ocular tissues as a consequence of aging and is present in high levels in drusen, Exp. Eye Res. 128 (2014) 151–155.
[6] S.K. Erickson, A.D. Cooper, S.M. Matsui, R.G. Gould, 7-Ketocholesterol. Its effects on hepatic cholesterogenesis and its hepatic metabolism in vivo and in vitro, J. Biol. Chem. 252 (1977) 5186–5193.
[7] N. Tamasawa, A. Tamasawa, K. Takebe, M. Hayakari, The effect of dietary 7-ketocholesterol, inhibitor of sterol synthesis, on hepatic microsomal cholesterol 7 alpha-hydroxylase activity in rat, Biochim. Biophys. Acta 1214 (1994) 20–26.
[8] M.A. Lyons, S. Samman, L. Gatto, A.J. Brown, Rapid hepatic metabolism of 7-ketocholesterol in vivo: implications for dietary oxysterols, J. Lipid Res. 40 (1999) 1846–1857.
[9] J.Y. Chiang, Bile acids: regulation of synthesis, J. Lipid Res. 50 (2009) 1955–1966.
[10] C.R. Pullinger, C. Eng, G. Salen, S. Shefer, A.K. Batta, S.K. Erickson, A. Verhagen, C.R. Rivera, S.J. Mulvihill, M.J. Malloy, J.P. Kane, Human cholesterol 7a-hydroxylase

(CYP7A1) deficiency has a hypercholesterolemic phenotype, J. Clin. Invest. 110 (2002) 109–117.
[11] M.A. Lyons, A.J. Brown, 7-Ketocholesterol delivered to mice in chylomicron remnant-like particles is rapidly metabolised, excreted and does not accumulate in aorta, Biochim. Biophys. Acta 1530 (2001) 209–218.
[12] M.A. Lyons, A.J. Brown, Metabolism of an oxysterol, 7-ketocholesterol, by sterol 27-hydroxylase in HepG2 cells, Lipids 36 (2001) 701–711.
[13] M.A. Lyons, N. Maeda, A.J. Brown, Paradoxical enhancement of hepatic metabolism of 7-ketocholesterol in sterol 27-hydroxylase-deficient mice, Biochim. Biophys. Acta 1581 (2002) 119–126.
[14] Z. Wu, K.O. Martin, N.B. Javitt, J.Y.L. Chiang, Structure and functions of human oxysterol 7alpha-hydroxylase cDNAs and gene CYP7B1, J. Lipid Res. 40 (1999) 2195–2220.
[15] J. Li-Hawkins, E.G. Lund, S.D. Turley, D.W. Russell, Disruption of the oxysterol 7alpha-hydroxylase gene in mice, J. Biol. Chem. 275 (2000) 16536–16542.
[16] H. Pettersson, J. Lundqvist, E. Oliw, M. Norlin, CYP7B1-mediated metabolism of 5alpha-androstane-3alpha,17beta-diol (3alpha-Adiol): a novel pathway for potential regulation of the cellular levels of androgens and neurosteroids, Biochim. Biophys. Acta 1791 (2009) 1206–1215.
[17] Y. Omoto, R. Lathe, M. Warner, J.A. Gustafsson, Early onset of puberty and early ovarian failure in CYP7B1 knockout mice, Proc. Natl. Acad. Sci. U. S. A. 102 (2005) 2814–2819.
[18] C.N. Falany, D. He, N. Dumas, A.R. Frost, J.L. Falany, Human cytosolic sulfotransferase 2B1: isoform expression, tissue specificity and subcellular localization, J. Steroid Biochem. Mol. Biol. 102 (2006) 214–221.
[19] H. Fuda, N.B. Javitt, K. Mitamura, S. Ikegawa, C.A. Strott, Oxysterols are substrates for cholesterol sulfotransferase, J. Lipid Res. 48 (2007) 1343–1352.
[20] C.N. Falany, K.J. Rohn-Glowacki, SULT2B1: unique properties and characteristics of a hydroxysteroid sulfotransferase family, Drug Metab. Rev. 45 (2013) 388–400 (Review).
[21] D.J. Waxman, Regulation of liver-specific steroid metabolizing cytochromes P450: cholesterol 7a-hydroxylase, bile acid 6ß-hydroxylase, and growth hormone-responsive steroid hormone hydroxylases, J. Steroid Biochem. Mol. Biol. 43 (1992) 1055–1072 (Review).
[22] N.E. Freeman, A.E. Rusinol, M. Linton, D.L. Hachey, S. Fazio, M.S. Sinensky, D.M. Thewke, Acyl-coenzyme A:cholesterol acyltransferase promotes oxidized LDL/oxysterol-induced apoptosis in macrophages, J. Lipid Res. 46 (2005) 1933–1943.
[23] S.S. Eveland, D.P. Milot, Q. Guo, Y. Chen, S.A. Hyland, L.B. Peterson, S. Jezequel-Sur, G.T. O'Donnell, P.D. Zuck, M. Ferrer, B. Strulovici, J.A. Wagner, W.K. Tanaka, D.A. Hilliard, O. Laterza, S.D. Wright, C.P. Sparrow, M.S. Anderson, A high-precision fluorogenic cholesteryl ester transfer protein assay compatible with animal serum and 3456-well assay technology, Anal. Biochem. 368 (2007) 239–249.
[24] A. Miyazaki, M. Sakai, Y. Sakamoto, S. Horiuchi, Acyl-coenzyme A:cholesterol acyltransferase inhibitors for controlling hypercholesterolemia and atherosclerosis, Curr. Opin. Investig. Drugs 4 (2003) 1095–1099 (Review).
[25] I.M. Larrayoz, J.D. Huang, J.W. Lee, I. Pascual, I.R. Rodriguez, 7-Ketocholesterol-induced inflammation is mediated by multiple kinase signaling pathways via NF {kappa}B but independently of reactive oxygen species formation, Invest. Ophthalmol. Vis. Sci. 51 (2010) 4942–4955.
[26] S. Cases, S. Novak, Y.W. Zheng, H.M. Myers, S.R. Lear, E. Sande, C.B. Welch, A.J. Lusis, T.A. Spencer, B.R. Karuse, S.K. Erickson, R.V. Farese Jr., ACAT-2, a second mammalian acyl-CoA:cholesterol acyltransferase. Its cloning, expression, and characterization, J. Biol. Chem. 273 (1998) 26755–26764.
[27] C.C. Chang, N. Sakashita, K. Ornvold, O. Lee, E.T. Chang, R. Dong, S. Lin, C.Y. Lee, S.C. Strom, R. Kashyap, J.J. Fung, R.V. Farese Jr., J.F. Patoiseau, A. Delhon, T.Y. Chang, Immunological quantitation and localization of ACAT-1 and ACAT-2 in human liver and small intestine, J. Biol. Chem. 275 (2000) 28083–28092.
[28] R.G. Lee, M.C. Willingham, M.A. Davis, K.A. Skinner, L.l. Rudel, Differential expression of ACAT1 and ACAT2 among cells within liver, intestine, kidney, and adrenal of nonhuman primates, J. Lipid Res. 41 (2000) 1991–2001.
[29] A. Linkous, E. Yazlovitskaya, Cytosolic phospholipase A2 as a mediator of disease pathogenesis, Cell. Microbiol. 12 (2010) 1369–1377 (Review).
[30] J.-D. Huang, J. Amaral, J.W. Lee, I.R. Rodriguez, 7-Ketocholesterol-induced inflammation signals mostly through the TLR4 receptor both in vitro and in vivo, PLoS One 9 (2014) e100985.
[31] C. Yu, J. Chen, S. Lin, J. Liu, C.C. Chang, T.Y. Chang, Human acyl-CoA:cholesterol acyltransferase-1 is a homotetrameric enzyme in intact cells and in vitro, J. Biol. Chem. 274 (1999) 36139–36145.
[32] I.A. Pikuleva, C.A. Curcio, Cholesterol in the retina: the best is yet to come, Prog. Retin. Eye Res. 41 (2014) 64–89.
[33] A. Kontush, HDL-mediated mechanisms of protection in cardiovascular disease, Cardiovasc. Res. 103 (2014) 341–349 (Review).